Available online at www.sciencedirect.com
ScienceDirect
Journal of Molecular Catalysis A: Chemical 260 (2006) 144–151
JOURNAL OF MOLECULAR CATALYSIS A: CHEMICAL
www.elsevier.com/locate/molcata

Oxidative dehydrogenation of ethane to ethylene over NiO loaded on high surface area MgO

Ken-Ichi Nakamura, Takanori Miyake, Toru Konishi, Toshimitsu Suzuki *

Department of Chemical Engineering and High Technology Research Center, Kansai University, Suita, Osaka 564-8680, Japan

Received 11 May 2006; received in revised form 14 June 2006; accepted 26 June 2006
Available online 22 August 2006

Abstract

The oxidative dehydrogenation of ethane over NiO-loaded MgO with high surface area was carried out using a fixed-bed flow reactor at 600 °C under atmospheric pressure.

At 600 °C, the oxidative dehydrogenation of ethane ($C_2H_6/O_2 = 1$) without dilution with an inert gas resulted in C_2H_6 conversion of 68.8% and a high C_2H_4 selectivity of 52.8%, which corresponds to a C_2H_4 yield of 36.3%. In addition, the catalytic activity did not decrease for at least 10 h. X-ray photoelectron spectra of the catalysts after the reaction exhibited that the initial valence state of Ni^{2+} (NiO) was maintained during the oxidative dehydrogenation of ethane. However, when NiO-loaded MgO was reduced with H_2 prior to the reaction, C_2H_4 selectivity decreased to nearly zero and high CO and H_2 selectivities were observed with the C_2H_6 conversion of 50 %, indicating that partial oxidation of C_2H_6 proceeded. Therefore, it seems important to keep Ni species as an oxide phase on the support, and for this purpose, use of the high surface area of MgO is essential.

Keywords: Dehydrogenation; Nickel oxide; Magnesium oxide

1. Introduction

Increasing demand on light alkenes is of current importance. Ethylene and propylene are the most important petrochemical feed stocks, and they are produced via steam cracking of naptha and the heavier fraction of natural gas. This process, however, is operated at a high temperature and consumes large amount of energy with low selectivities to alkenes and unavoidable coke formation [1].

Recently, an efficient utilization of light gases from oil fields has attracted a great deal of attention from petrochemical industries, and as a result, intensive development of more efficient and selective processes has been carried out. One of such processes is an oxidative dehydrogenation of ethane to ethylene (ODHE; reaction (1)):

$$C_2H_6 + \tfrac{1}{2}O_2 \rightarrow C_2H_4 + H_2O, \quad \Delta H^\circ_{298} = -149\,\text{kJ/mol} \tag{1}$$

Oxidative dehydrogenation of ethane to ethylene could be achieved at much lower temperatures than those with steam cracking due to an exothermic reaction.

Catalytic oxidative dehydrogenation of ethane was first reported by Lunsford et al. over MoO_3 on SiO_2 using N_2O as an oxidant [2]. A large number of researchers have proposed various catalysts effective for ODHE; they are classified as non-reducible catalysts, reducible metal-oxide catalysts and complex metal-oxide catalysts.

Aika et al. [3] have shown that Co^{2+}-doped MgO is effective for the ODHE with N_2O as an oxidant. However, it is difficult to industrialize this process because of the high cost of N_2O as an oxidant. From an industrial viewpoint, catalytic oxidative dehydrogenation of ethane using oxygen as an oxidant should be exploited.

Thorsteinson et al. [4] have reported that mixed oxide of Mo and V is active for the ODHE, with very high selectivity to ethylene with a low conversion.

Lunsford et al. reported that Li^+/MgO catalyst was active in the oxygen and ethane mixed gas at a low O_2 partial pressure. They proposed that ethoxide formed on MgO surface via ethyl radicals afforded a high yield of ethylene up to 34% at a reaction

* Corresponding author. Fax: +81 6 6388 8869.
E-mail address: tsuzuki@ipcku.kansai-u.ac.jp (T. Suzuki).

1381-1169/$ – see front matter © 2006 Elsevier B.V. All rights reserved.
doi:10.1016/j.molcata.2006.06.058

temperature above 600 °C [5,6]. However, the catalyst exhibited only a short lifetime.

The ODHE reaction over V_2O_5- or MoO_3-loaded catalysts has achieved high ethylene selectivity via the redox cycle (Mars and Krevelen mechanism) and/or acid–base properties [7–10]. However, a high activity always proceeded with deep oxidation of produced ethylene.

Layered complex metal chloride oxide $SrBi_3O_4Cl_3$ with $SrCl_2$ and KCl afforded very high selectivity to ethylene in the reaction of ethane and oxygen at 660 °C [11,12].

Non-reducible mixed metal oxides like Mo–V–Te oxides for ODHE have been reported to exhibit high activity at a temperature lower than 400 °C [13–17]. In these studies, most of the researchers employed conditions in which ethane and oxygen were highly diluted with an inert gas. From a practical stand point, dilution with inert gases must be avoided.

We have reported that carbon dioxide, as a mild oxidant, markedly promotes the dehydrogenation of ethane over Ga_2O_3-loaded TiO_2 and Cr_2O_3-loaded oxidized diamond catalysts [18,19]. However, with these catalyst systems, ethylene yields decreased with an increase in the reaction time, due to carbon deposition onto the catalyst. To overcome this, development of an active and selective new catalyst using oxygen as an oxidant is essential.

Recently, NiO-loaded on Al_2O_3 catalysts for ODHE have been reported to exhibit high activity [20–22]. NiO-loaded Al_2O_3 catalyst with highly dispersed NiO produces a high yield of ethylene. However, details regarding active sites for ODHE have not yet been clarified. Heracleous et al. have reported that Nb for NiO–Nb_nO_m catalyst improves the dispersion of the nickel phase and facilitates C–H bond activation by acting as an electron transfer promoter [23,24].

Heracleous et al. have reported that in the comparison between V- or Mo-oxide loaded on Al_2O_3 and those loaded on TiO_2, the presence of basic sites enhances the fast desorption of the produced olefins on the catalyst surface, resulting in higher selectivities [10]. However, NiO loaded on basic support for ODHE has not been reported. Ruckenstein et al. have described that Ni species loaded on MgO catalyst exist in the form of a solid solution, which stabilizes nickel against sintering during the CO_2 reforming of methane [25,26]. This finding seems to indicate that the highly dispersed NiO loaded on high-surface area MgO would be resistant to sintering and would promote the ODHE.

The present study focused on the ODHE on NiO-loaded catalysts without dilution with an inert gas, and here we report that MgO with high surface area is a promising support for this reaction.

2. Experimental

2.1. Catalyst preparation

The catalyst supports used in this study were MgO (100, 1000 A; Ube Industries Ltd.), Al_2O_3 (Sumitomo Chemical Co.), SiO_2 (Wako Pure Chemical Industries Ltd.), TiO_2 (P25; Japan Aerosil Co.), La_2O_3, and Y_2O_3 (Nacalai Tesque, Inc.).

The supported nickel oxide catalysts containing 5 wt.% of Ni as metal were prepared by impregnating an ethanol solution of $Ni(acac)_2$ (Nacalai Tesque, Inc.) to a suspended support, followed by evaporation-to-dryness under vacuum. Supported catalyst precursors were calcined at 600 °C for 5 h in air prior to the reaction. After the calcination, the catalysts were crashed and sieved to pass a 100 mesh screen and used for the reaction.

2.2. Catalytic reaction

The oxidative dehydrogenation of ethane was carried out with a fixed-bed flow-type quartz reactor (8 mm i.d. × 350 mm *L*) at a temperature range from 450 to 600 °C under atmospheric pressure. After placing 60 mg of a catalyst in the reactor, O_2 and C_2H_6 were introduced with a molar ratio from 1:2 to 1:1. The total gas flow rate was fixed at 30 mL/min. Effluent gas (H_2, CO, CO_2, CH_4, C_2H_4, C_2H_6 and O_2) was analyzed with an online high-speed gas chromatograph equipped with TCD detectors (PC-Chrom, M200 Chromato Analyzer) using Molecular Sieve 5 A and Poraplot Q columns.

2.3. Catalyst characterization

The surface area of the support and catalyst was measured by the BET method using N_2 at 77 K with an automatic Micromeritics Gemini 2375.

Temperature programmed reduction (TPR) was performed using an online quadrupole mass spectrometer (HAL201, Hiden Analytical Ltd.) fitted with an outlet of a fixed-bed quartz reactor (i.d. 4 mm × 200 mm). After placing a 50 mg of catalyst in the reactor, 3 mL/min of H_2 and 27 mL/min of Ar were introduced. Before the reaction, the catalyst was pretreated under Ar flow for 30 min at 400 °C. A mass spectrometer was scanned for corresponding parent peaks of the following five compounds, H_2, H_2O, CH_4, CO, and CO_2, within 1 s, and repeated scans were collected on a personal computer.

Pulsed CO adsorption technique was employed to measure the amounts of CO adsorbed on Ni by using a home build apparatus.

X-ray photoelectron spectroscopy (XPS) was obtained on an X-ray photoelectron spectrometer (Jeol JPS-9000MX) using Mg Kα radiation as the energy source with the reference of C 1s at 285.0 eV

A Jeol JEM2010 was used to obtain high-resolution transmission electron microscope (HR-TEM) images at 200 kV.

3. Results and discussion

3.1. Activities of NiO-loaded catalysts in the oxidative dehydrogenation of ethane

Table 1 summarizes the effects of various supports on ODHE at 600 °C. As seen in Run 1, even without catalyst ODHE slightly proceeded to give an ethylene yield of 5%. NiO loaded on Al_2O_3, SiO_2, Y_2O_3, La_2O_3, and TiO_2 and low-surface area MgO (LS-MgO) (Runs 2–8) afforded high C_2H_6 conversions with high CO and H_2 selectivities. This finding indicates that partial oxidation

Table 1
Effect of various supports on the oxidative dehydrogenation of ethane

Run	Support	Support surface area (m^2/g)	C_2H_6 conversion (%)	C_2H_4 yield (%)	Selectivity (%)					Carbon (mg)
					C_2H_4	CO	CO_2	H_2	CH_4	
1	No catalyst	–	4.7	4.7	99.0	0.0	0.7	0.8	0.0	–
2	Al_2O_3	152	32.0	0.1	0.3	46.4	51.7	67.7	1.6	19.4
3	SiO_2	199	46.5	0.1	0.2	39.9	36.1	40.9	23.9	8.5
4	CaO	6	45.2	0.0	0.1	42.2	36.6	55.5	21.2	150.4
5	Y_2O_3	15	44.9	0.1	0.2	55.0	28.8	60.1	16.0	98.0
6	La_2O_3	4	53.4	0.1	0.1	51.0	26.8	50.0	22.1	74.3
7	TiO_2	50	35.4	0.2	0.5	60.9	30.6	66.1	8.1	78.8
8	LS-MgO[a]	17	40.4	0.1	0.2	63.1	32.0	73.6	4.7	18.4
9	HS-MgO[b]	145	32.0	17.4	54.3	10.3	32.2	13.3	3.2	–
10	HS-MgO[c]	145	68.8	36.3	52.8	8.4	32.9	10.6	5.9	–
11	HS-MgO[d]	145	49.6	0.0	0.1	47.0	32.3	55.7	20.7	90.2

Catalyst: Ni loading level 5 wt.%, 60mg; reaction temperature: 600 °C; reaction time: 1 h; flow rate: C_2H_6/O_2 = 20 mL/min/10 mL/min; space velocity: 30,000 mL/g cat h.
[a] LS: low surface area.
[b] HS: high surface area.
[c] O_2 partial pressure: 50.7 kPa, C_2H_6/O_2 15 mL/min/15 mL/min.
[d] Pretreatment: H_2 20 mL/min, 600 °C, 1 h.

of ethane to CO and H_2 proceeded (POE; reaction (2)). There was also carbon formation on these supports as a side reaction:

$$C_2H_6 + O_2 \rightarrow 2CO + 3H_2, \quad \Delta H^{\circ}_{298} = -136\,\text{kJ/mol} \qquad (2)$$

In order to confirm the Ni species after the reaction, XRD of the catalysts were measured, as shown in Fig. 1. After the reaction, NiO loaded on Al_2O_3 showed neither NiO nor Ni. On the other hand, after the reaction using the other supports, diffraction peaks ascribed to metallic Ni were observed. This finding indicates that NiO on these supports was reduced to metallic Ni by the feed C_2H_6 and produced H_2, and the POE reaction then proceeded on these catalysts.

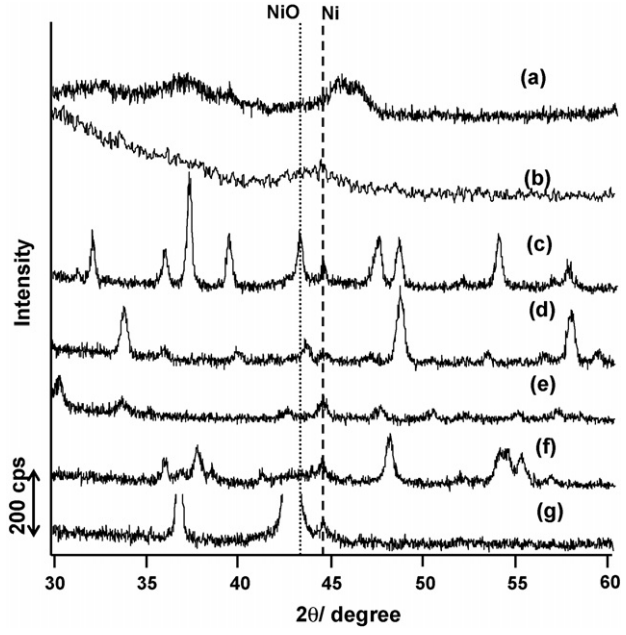

Fig. 1. XRD patterns of NiO-loaded catalysts after the reaction. (a) NiO/Al_2O_3; (b) NiO/SiO_2; (c) NiO/CaO; (d) NiO/Y_2O_3; (e) NiO/La_2O_3; (f) NiO/TiO_2; (g) NiO/LS-MgO. Strong peaks are diffraction peaks of support materials.

When MgO having high surface area (HS-MgO) was employed as a support, C_2H_6 conversion decreased to 32.0% with a high C_2H_4 selectivity of 54.3%, and C_2H_4 yield of 17.4% was obtained without carbon formation (Run 9). As discussed later, at a high partial pressure of O_2, C_2H_4 yield of 36.8% was obtained (Run 10). From these findings, high-surface area MgO was selected as the best support material for NiO in the ODHE and used in the following detailed studies.

If NiO-loaded HS-MgO was reduced with H_2 prior to the reaction, C_2H_4 selectivity decreased to nearly zero, although C_2H_6 conversion increased to 50% (Run 11). These results seem to indicate that dehydrogenation proceeded on NiO, while only POE proceeded on metallic Ni.

In order to confirm active species of NiO loaded on HS-MgO, X-ray photoelectron spectra of various Ni-loaded catalysts are compared and are shown in Fig. 2. It is known that the Ni $2p_{2/3}$ peak of bulk NiO and that of metallic Ni appear at 853.5 and 852.9 eV, respectively. On the surface of the fresh catalyst (Fig. 2a), only NiO was observed, as evidenced by the single peak at 853.3 eV, and after H_2 reduction at 600 °C the binding energy of Ni $2p_{2/3}$ shifted to the lower binding energy side, indicating that NiO was reduced to metallic Ni (Fig. 2b). The spectrum of the catalyst after the ODHE reaction with C_2H_6 and O_2 (2:1) showed an overlapping peak composed of both NiO and metallic Ni (Fig. 2c). On the other hand, only a peak ascribed to metallic Ni was observed after the reaction with the pre-reduced catalyst (Fig. 2d).

NiO and MgO are well known to form solid solution. Parmalaina et al. have reported that a high calcination temperature at 800 °C favors the diffusion of NiO on the surface of MgO to the inside of the MgO lattice to form solid solution [27]. It is reported to be difficult to reduce once formed NiO–MgO solid solution on the MgO surface by H_2 [28].

H_2-TPR patterns of the NiO loaded on HS-MgO catalyst at various calcination temperatures are presented in Fig. 3. With NiO/HS-MgO calcined at 400 °C, weak broad response of H_2O

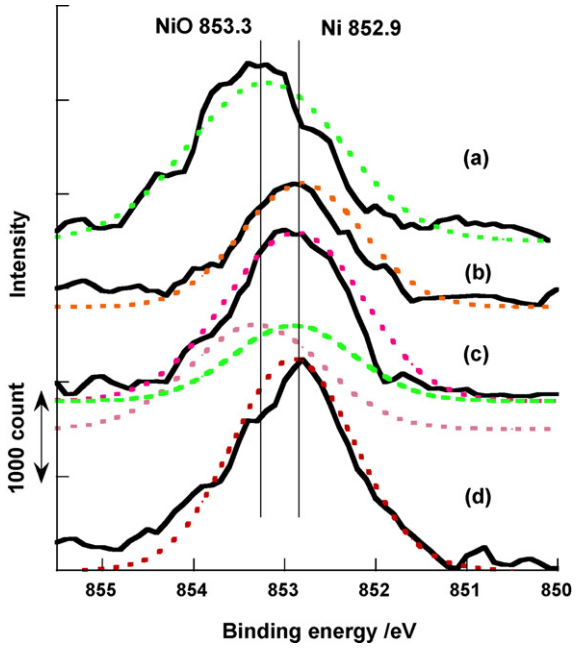

Fig. 2. X-ray photoelectron spectra of NiO/HS-MgO catalysts. (a) Fresh catalyst; (b) fresh catalyst was H_2 reduced at 600 °C for 1 h; (c) catalyst after the ODHE at 600 °C for 1 h with $C_2H_6/O_2 = 2$; (d) H_2-reduced catalyst after the ODHE at 600 °C for 1 h with $C_2H_6/O_2 = 2$.

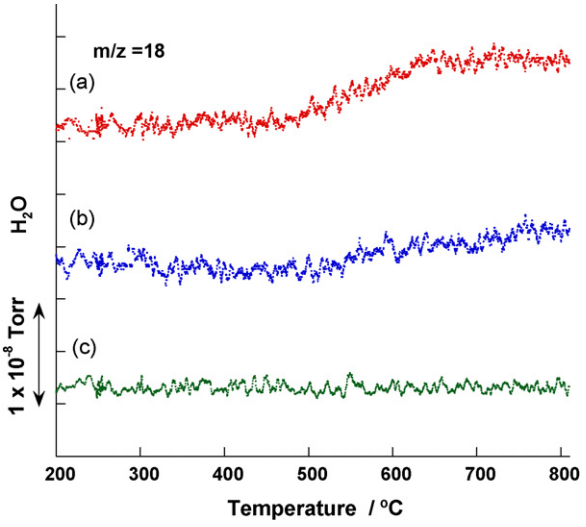

Fig. 3. H_2-temperature-programmed reduction patterns of NiO/HS-MgO catalysts calcined at various temperatures. (a) Calcination temperature: 400 °C; (b) calcination temperature: 600 °C; (c) calcination temperature: 950 °C. Ramping rate: 10 °C/min, Ar = 27 mL/min, H_2 = 3 mL/min, Ni loading level 5 wt.% as metal, Pretreatment before TPR: Ar = 27 mL/min, 400 °C, 30 min.

appeared from 500 to 800 °C, and with that calcined at 600 °C afforded weaker response, indicating that on both of the catalysts, NiO species existed on MgO (Fig. 2a and b). On the other hand, for the NiO/HS-MgO calcined at 950 °C, no distinct reduction peak was observed, suggesting that the amount of NiO decreased on the MgO surface, probably due to the formation of a NiO–MgO solid solution.

Table 2 illustrates the effects of catalyst calcination temperature on the C_2H_6 conversion and product selectivities. With NiO-loaded HS-MgO calcined at 400 °C, the C_2H_6 conversion of 40.4% was obtained with high selectivities to CO and H_2. This finding indicates that NiO on HS-MgO was reduced to metallic Ni and the POE proceeded. On the other hand, with NiO/HS-MgO calcined at 600 °C, the C_2H_6 conversion decreased to 32.0% with a high C_2H_4 selectivity of 54.3%. With NiO/HS-MgO calcined at 950 °C, the C_2H_6 conversion further decreased to 22.8% with a decrease in C_2H_4 selectivity to 28.5%. These results suggest that the interaction is weak between NiO and MgO in the NiO-loaded MgO catalyst calcined at 400 °C, and that NiO would be reduced to some extent to metallic Ni, giving CO and H_2 via the POE. On the other hand, calcination at 600 °C, the peripheral portion of NiO particles on the MgO surface could form a NiO–MgO solid solution, but the central portion of the particles would remain as NiO. On the NiO surface, the ODHE reaction might have proceeded to give ethylene, as indicated by the decrease in the intensity of H_2O desorption in the H_2-TPR.

To evaluate sizes and the amount of reducible NiO on MgO after calcination, the calcined catalysts were hydrogen reduced at 400 °C, and then CO adsorption was measured by pulse technique. The results are shown in Table 2. The amount of CO adsorbed decreased with an increase in the calcination temperature, indicating that loss of reducible NiO and increase in the particle sizes.

3.2. Effects of Ni-loading level on the ODHE

Table 3 illustrates the effects of Ni-loading level on the C_2H_6 conversion and product selectivities. Over bare support MgO (Run 15), ethane conversion and product selectivity were similar to those without catalyst (Run 1). With an increase in the Ni-loading level, from 1 to 3 wt.%, C_2H_6 conversion and C_2H_4 selectivity markedly increased. Zhang et al. stated that well dispersed NiO on Al_2O_3 is effective for the ODHE [20]. It seems natural to predict that at a lower Ni-loading level C_2H_4 selectivity increases with a decrease in the selectivity to CO_2, since the lower loading level provides higher dispersion of NiO on

Table 2
Effect of calcination temperature of the catalyst on the oxidative dehydrogenation of ethane

Run	Calcination (°C)	Surface area (m^2/g)	CO adsorption[a] (μmol/g cat)	C_2H_6 conversion (%)	C_2H_4 yield (%)	Selectivity (%)				
						C_2H_4	CO	CO_2	H_2	CH_4
12	400	101	29.9	40.4	0.1	0.2	63.1	32.0	73.3	4.7
13	600	84	17.4	32.0	17.4	54.3	10.3	32.2	13.3	3.2
14	950	23	5.4	22.8	6.5	28.5	4.8	65.1	0.7	1.6

Catalyst: 60 mg; reaction temperature: 600 °C; reaction time: 1 h; flow rate: C_2H_6/O_2 = 20 mL/min/10 mL/min; space velocity: 30,000 mL/g cat h.
[a] CO adsorption was carried out at 25 °C, after reducing the calcined catalyst at 400 °C for 1 h.

Table 3
Effect of Ni-loading level on the oxidative dehydrogenation of ethane

Run	Ni (wt.%)	Surface area (m^2/g)	C_2H_6 conversion (%)	C_2H_4 yield (%)	Selectivity (%)				
					C_2H_4	CO	CO_2	H_2	CH_4
15	0	145	6.1	5.4	88.6	4.3	7.1	6.4	0.0
16	1	84	20.3	4.2	20.8	7.7	70.8	0.4	0.8
17	2	80	23.5	8.0	34.0	7.9	57.1	0.1	1.0
18	3	85	31.3	16.4	52.3	12.2	32.5	16.5	3.0
19	5	74	32.0	17.4	54.3	10.3	32.2	13.3	3.2
20	10	52	33.3	16.4	49.3	7.9	38.9	11.1	3.8
21	15	–	52.1	0.0	0.1	57.3	24.2	58.8	18.4

Catalyst: 60 mg; reaction temperature: 600 °C; reaction time: 1 h; flow rate: C_2H_6/O_2 = 20 mL/min/10 mL/min; space velocity: 30,000 mL/g cat h.

the MgO surface. However, in our case, an increase in the NiO-loading level increased the C_2H_4 selectivity with a decrease in CO_2 selectivity.

With an increase in Ni-loading level from 3 to 10 wt.%, however, C_2H_6 conversion and C_2H_4 selectivity remained constant with a slight increase in CO_2 selectivity. If the NiO-loading level was increased to 15 wt.%, however, the C_2H_4 selectivity decreased to nearly zero with 50% C_2H_6 conversion. At a high NiO-loading level, the particle size of NiO on HS-MgO becomes larger, so that the interaction between NiO and HS-MgO would decrease to undergo facile reduction to metallic Ni. As a result, POE proceeded at a higher Ni-loading level. From these results, the optimal loading level of Ni for HS-MgO would be 5 wt.%.

3.3. Effects of reaction temperature on the ODHE

Fig. 4 shows the effects of reaction temperature on the ODHE over NiO loaded on HS-MgO catalyst. Below 450 °C, the reaction did not proceed and the ODHE occurred at above 475 °C. With increases in reaction temperature, the C_2H_6 conversion and C_2H_4 selectivity increased with a decrease in the CO_2 selectivity. One of the most undesired problems associated with the ODHE catalysts is the decrease in the olefin selectivity with increasing alkane conversion, consistent with parallel-consecutive reactions [10]. Alkene is highly reactive molecule, in most cases more reactive than the corresponding alkane. Alkene is easily activated on the catalyst surface and undergoes secondary oxidation reactions to CO_x. In the case of NiO loaded on HS-MgO catalyst, the C_2H_4 selectivity increased with an increase in the reaction temperature up to 625 °C.

When the oxidation of C_2H_4 was carried out without catalyst using the same reactor at 550 °C, the main products were CO and CO_2 with a high C_2H_4 conversion of 30%, indicating that C_2H_4 and unreacted O_2 easily reacted to give CO_2. With an increase in the reaction temperature, the formation rate of C_2H_4 seems to be higher than the secondary oxidation rate of C_2H_4. Another possible reason for the increased selectivity of C_2H_4 at a higher reaction temperature is the decrease in the concentration of unreacted O_2, due to the increase in the C_2H_6 conversion. With increases in the reaction temperature, the C_2H_4 selectivity therefore increased with a decrease in the CO_2 selectivity.

3.4. Effects of O_2 partial pressure and space velocity on the ODHE

Fig. 5 shows the effects of the O_2 partial pressure on the ODHE over NiO loaded on HS-MgO catalyst, keeping the total gas flow rate at 30 mL/min. The O_2/C_2H_6 ratio was varied from 0.33 to 1. At an O_2/C_2H_6 ratio of 1, the highest C_2H_6 conversion and C_2H_4 yield were obtained. However, at a lower O_2 partial pressure, CO_2, CO, and H_2 selectivities increased, with a decrease in the selectivity to C_2H_4. This is just opposite behavior observed in general oxidative selective reactions, where under a low O_2/substrate ratio, selectivity to the desired

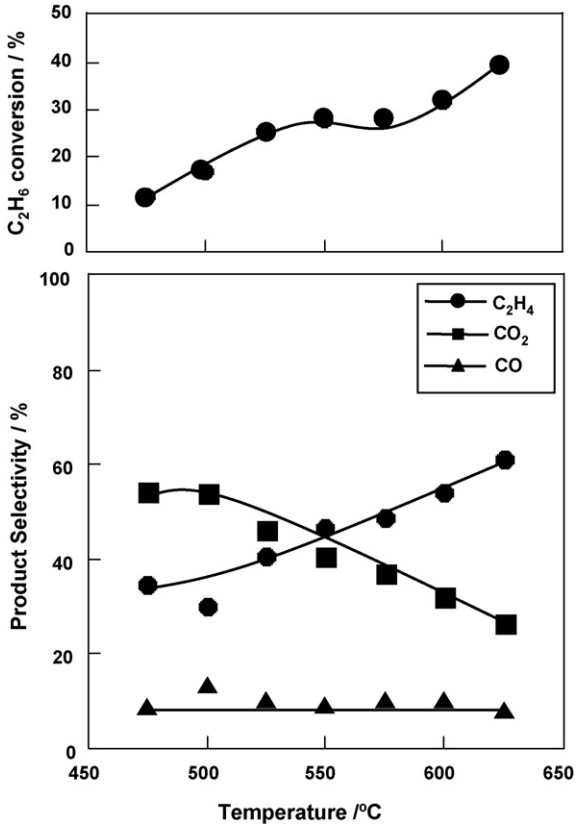

Fig. 4. Effects of reaction temperature on the C_2H_6 conversion and product selectivity over NiO/HS-MgO in the oxidative dehydrogenation of ethane. Catalyst: 60 mg; flow rate: 30 mL/min (C_2H_6/O_2 = 0.5); space velocity: 30,000 mL/g cat h; Ni loading level: 5 wt.%.

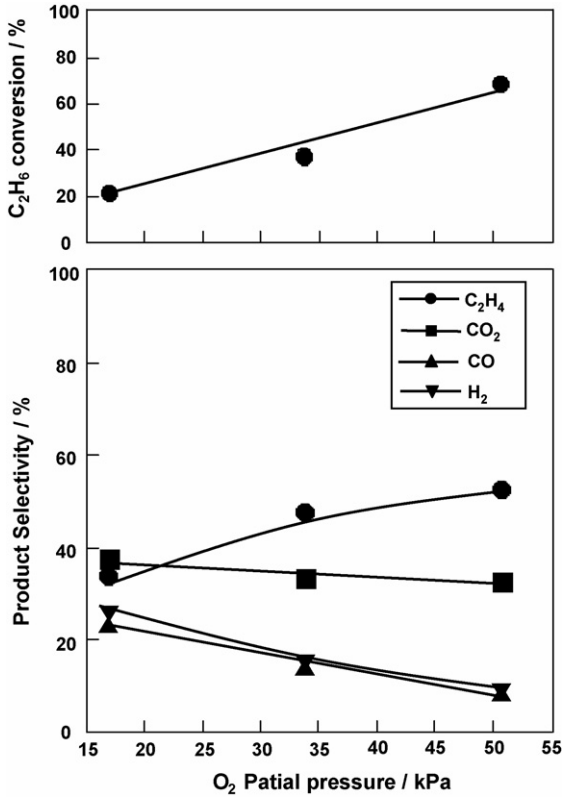

Fig. 5. Effects of O_2 partial pressure on the C_2H_6 conversion and product selectivity over NiO/HS-MgO in the oxidative dehydrogenation of ethane. Catalyst: 60 mg; flow rate: 30 mL/min; reaction temperature: 600 °C; space velocity: 30,000 mL/g cat h; Ni loading level: 5 wt.%; total pressure: 0.1 MPa.

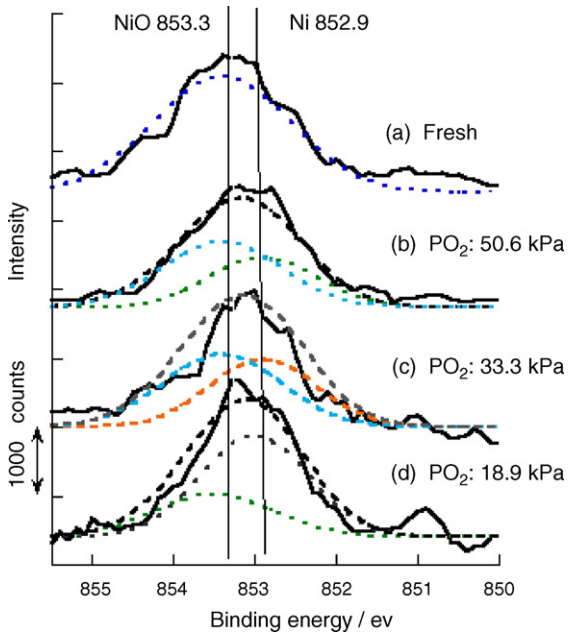

Fig. 6. X-ray photoelectron spectra of NiO/HS-MgO catalyst after the reaction at various C_2H_6/O_2 ratios. (a) Fresh catalyst; (b) catalyst after the reaction at $PO_2 = 50.6$ kPa; (c) catalyst after the reaction at $PO_2 = 33.8$ kPa; (d) catalyst after the reaction at $PO_2 = 16.9$ kPa. Other conditions are the same as Fig. 5.

product increases. Accordingly, at the lower O_2 partial pressure, NiO on HS-MgO would be reduced to metallic Ni due to the reducing atmosphere, and CO and H_2 selectivities increased according to the progress of the POE.

These results were confirmed by XPS analyses of the catalysts before and after the reaction under different oxygen partial pressures (Fig. 6). With a decrease in the O_2 partial pressure, the binding energy of Ni $2p_{3/2}$ peaks shifted to lower values, and the deconvoluted peak area ratio of Ni(II) to Ni(0) increased one to three, indicating that NiO on the fresh catalyst tended to be reduced to metallic Ni by the feed of C_2H_6 rich gas.

Fig. 7 shows the effects of the space velocity on the ODHE over NiO loaded on HS-MgO catalyst. The space velocity was varied by changing the amount of catalyst in the reactor. With an increase in the space velocity from 25,000 to 180,000 mL/g cat h, the C_2H_4 selectivity increased from 54.3 to 65.1% with a decrease in the C_2H_6 conversion from 35.6 to 16.7%. C_2H_4 selectivity decreased with an increased contact time due to the secondary deep oxidation reaction of C_2H_4 to CO_2 and H_2O.

3.5. Stability of NiO loaded on HS-MgO catalyst in the ODHE

Catalytic performance of NiO loaded on HS-MgO catalyst was tested for a prolonged period at 600 °C at an O_2/C_2H_6 ratio of 0.5. Fig. 8 shows the conversion of C_2H_6 and the C_2H_4,

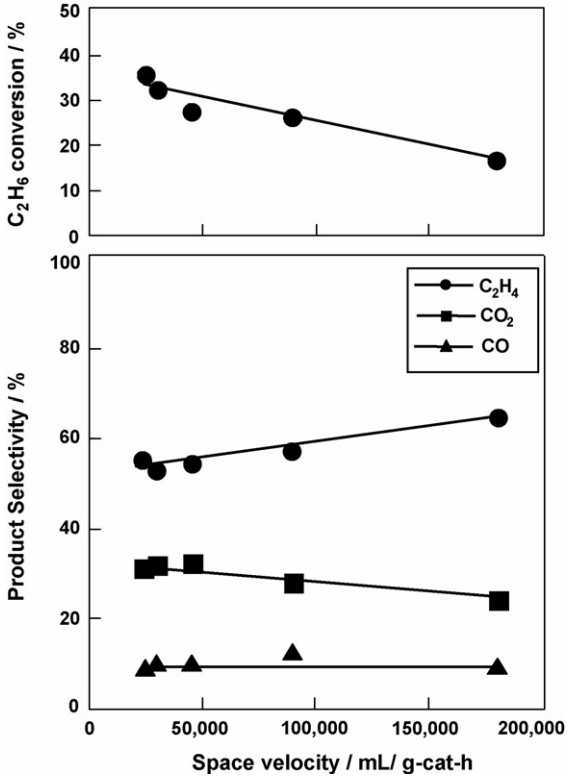

Fig. 7. Effects of space velocity on the C_2H_6 conversion and product selectivity over NiO/HS-MgO in the oxidative dehydrogenation of ethane. Catalyst: 5–72 mg; flow rate: 30 mL/min ($C_2H_6/O_2 = 0.5$); reaction temperature: 600 °C; Ni loading level: 5 wt.%.

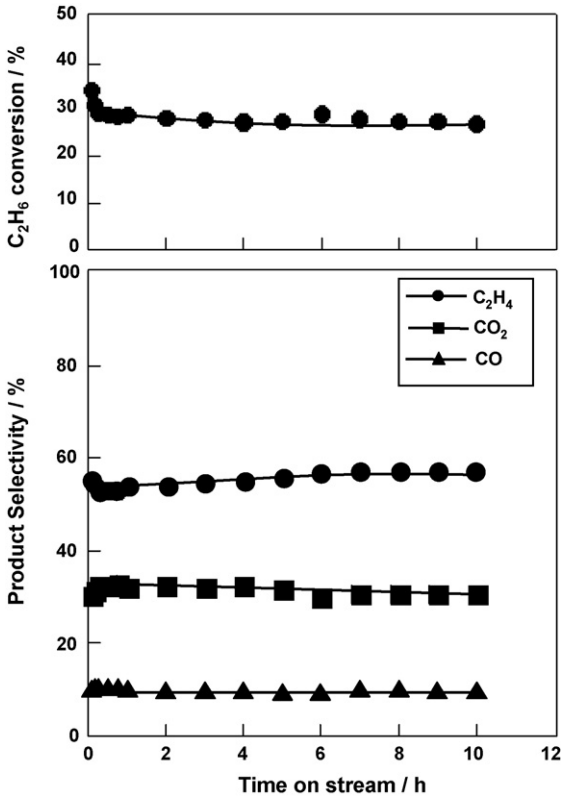

Fig. 8. Catalytic activity and product selectivity in the ODHE against time on stream over NiO/HS-MgO. Catalyst: 60 mg; flow rate: 30 mL/min (C_2H_6/O_2 = 0.5); reaction temperature: 600 °C; space velocity: 30,000 mL/g cat h; Ni loading level: 5 wt.%.

CO_2, and CO selectivities as a function of time on stream. As time progressed, the C_2H_6 conversion decreased slightly with an increase in the C_2H_4 selectivity. These results indicate that the catalyst may exhibit high activity for prolonged period.

3.6. HR-TEM images of NiO loaded on MgO catalyst

Fig. 9 shows HR-TEM images of NiO loaded on HS-MgO catalyst. TEM images of MgO crystallites were cubic, and considerably uniform and darker NiO images of ca 7 nm were seen. The well dispersed NiO observed by TEM images provides strong evidence of the higher performance of NiO loaded on HS-MgO catalyst for the selective ODHE to ethylene.

4. Conclusion

For the oxidative dehydrogenation of ethane to ethylene (ODHE), NiO catalyst loaded on high-surface area MgO (HS-MgO) afforded high C_2H_6 conversion of 68.8%, C_2H_4 selectivity of 52.8%, and C_2H_4 yield of 36.8% at 600 °C, without dilution of the feed.

XRD, XPS, and H_2-TPR revealed that NiO phase surrounded by NiO–MgO solid solution was the active phase for the ODHE. To keep Ni species as NiO, a high surface area of MgO was essential. When the NiO was reduced to metallic Ni, the partial oxidation of ethane proceeded with high selectivity to CO and H_2.

HR-TEM images showed that the NiO particle size on high-surface area MgO was around 7 nm. Thus, highly dispersed NiO on HS-MgO is effective for the ODHE.

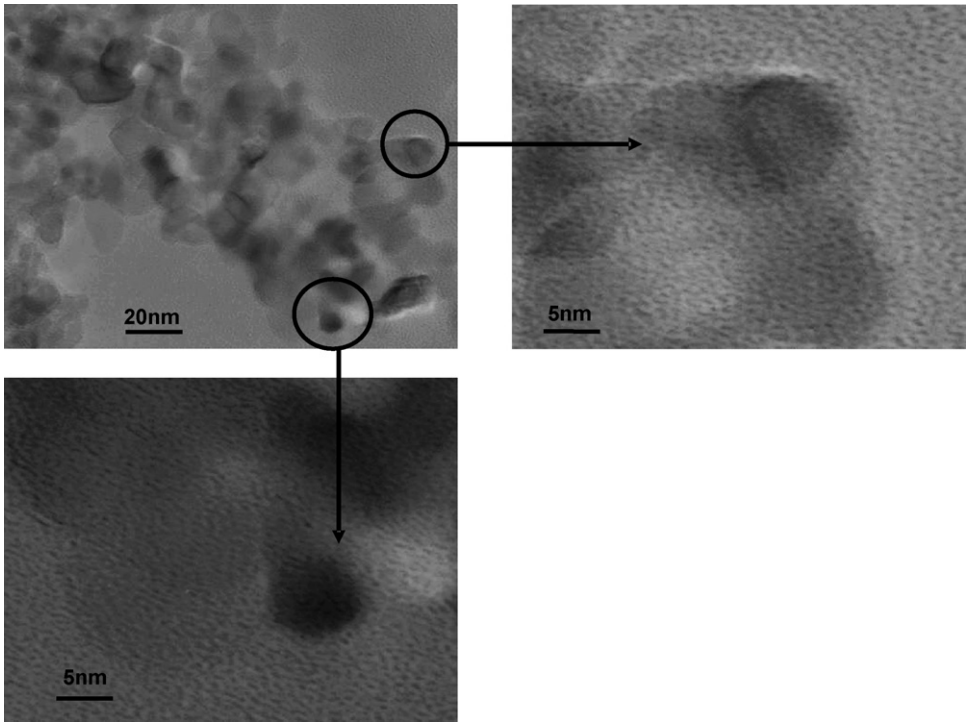

Fig. 9. TEM images of NiO/HS-MgO catalyst. Upper left: whole image, upper right and bottom: enlarged images.

Acknowledgements

This work was supported in part by the "High-Tech Research Center" Project for Private Universities: matching fund subsidy from MEXT (Ministry of Education, Culture, Sports, Science and Technology), 2001–2006 and grant-in-aid for Scientific Research (B) from Japan Society for the Promotion of Science.

References

[1] C.J. Pereira, Science 285 (1999) 670.
[2] M.B. Ward, M.J. Lin, J.H. Lunsford, J. Catal. 50 (1977) 306.
[3] K. Aika, M. Isobe, K. Kido, T. Moriyama, T. Onishi, J. Chem. Soc., Faraday Trans. 83 (1987) 3139.
[4] E.M. Thorsteinson, T.P. Wilson, F.G. Young, P.H. Kasai, J. Catal. 52 (1978) 116.
[5] E. Morales, J.H. Lunsford, J. Catal. 118 (1989) 255.
[6] S.J. Conway, J.H. Lunsford, J. Catal. 131 (1991) 513.
[7] M.D. Argyle, K. Chen, A.T. Bell, E. Iglesia, J. Catal. 208 (2002) 139.
[8] B. Solsona, V.A. Zazhigalov, J.M. López Nieto, I.V. Bacherikova, E.A. Diyuk, Appl. Catal. A: Gen. 249 (2003) 81.
[9] M.P. Casaletto, L. Lisi, G. Mattogno, P. Patrono, F. Pinzari, G. Ruoppolo, Catal. Today 91/92 (2004) 271.
[10] E. Heracleous, M. Machli, A.A. Lemonidou, I.A. Vasalos, J. Mol. Catal. A: Chem. 232 (2005) 29.
[11] W. Ueda, S.-W. Lin, I. Tohmoto, Catal. Lett. 44 (1997) 241.
[12] S.-W. Lin, Y.-C. Kim, W. Ueda, Bull. Chem. Soc. Jpn. 71 (1998) 1089.
[13] J.M. López Nieto, P. Botella, M.I. Vázquez, A. Dejoz, Chem. Commun. (2002) 1906.
[14] P. Botella, E. García-González, A. Dejoz, J.M. López Nieto, M.I. Vázquez, J. González-Calbet, J. Catal. 225 (2004) 428.
[15] W. Ueda, N.-F. Chen, K. Oshihara, Chem. Commun. (1999) 517.
[16] W. Ueda, K. Oshihara, Appl. Catal. A: Gen. 200 (2000) 135.
[17] J.M. López Nieto, P. Botella, P. Concepción, A. Dejoz, M.I. Vázquez, Catal. Today 91/92 (2004) 241.
[18] K. Nakagawa, C. Kajita, K. Okumura, N. Ikenaga, M. Nishitani-Gamo, T. Ando, T. Kobayashi, T. Suzuki, J. Catal. 203 (2001) 87.
[19] K. Nakagawa, C. Kajita, N. Ikenaga, T. Suzuki, T. Kobayashi, M. Nishitani-Gamo, T. Ando, J. Phys. Chem. B 107 (2003) 4048.
[20] X. Zhang, J. Liu, Y. Jing, Y. Xie, Appl. Catal. A: Gen. 240 (2003) 143.
[21] E. Heracleous, A.F. Lee, K. Wilson, A.A. Lemonidou, J. Catal. 231 (2005) 159.
[22] X. Zhang, Y. Gong, G. Yu, Y. Xie, J. Mol. Catal. A: Chem. 180 (2002) 293.
[23] E. Heracleous, A.A. Lemonidou, J. Catal. 237 (2006) 162.
[24] E. Heracleous, A.A. Lemonidou, J. Catal. 237 (2006) 175.
[25] E. Ruckenstein, Y.H. Hu, Ind. Eng. Chem. Res. 37 (1998) 1744.
[26] Y. Hu, E. Ruckenstein, Catal. Lett. 36 (1996) 145.
[27] A. Parmalina, F. Arena, F. Frusteri, N. Giordano, J. Chem. Soc., Faraday Trans. 86 (1990) 2663.
[28] D. Xu, W. Li, Q. Ge, H. Xu, Fuel Process. Technol. 86 (2005) 99.